

Reactivity-Based Probe of the Iron(II)-Dependent Interactome Identifies New Cellular Modulators of Ferroptosis

Ying-Chu Chen, Juan A. Osés-Prieto, Lauren E. Pope, Alma L. Burlingame, Scott J. Dixon, and Adam R. Renslo*

Cite This: <https://dx.doi.org/10.1021/jacs.0c06709>

Read Online

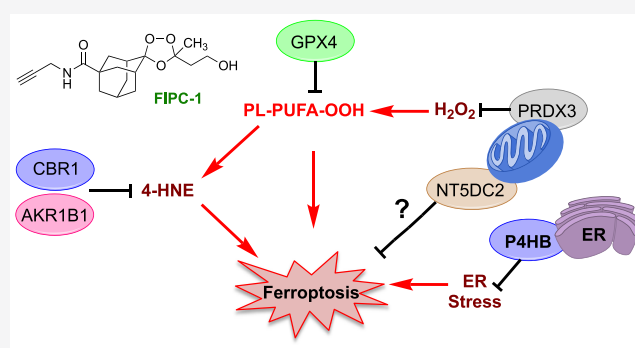
ACCESS |

Metrics & More

Article Recommendations

Supporting Information

ABSTRACT: Ferroptosis is an iron-dependent form of cell death resulting from loss or inhibition of cellular machinery that protects from the accumulation of lipid hydroperoxides. Ferroptosis likely serves a tumor suppressing function in normal cellular homeostasis, but certain cancers exploit and become highly dependent on specific nodes of the pathway, presumably to survive under conditions of increased oxidative stress and elevated labile ferrous iron levels. Here we introduce Ferroptosis Inducing Peroxide for Chemoproteomics-1 (FIPC-1), a reactivity-based probe that couples Fenton-type reaction with ferrous iron to subsequent protein labeling via concomitant carbon-centered radical generation. We show that FIPC-1 induces ferroptosis in susceptible cell types and labels cellular proteins in an iron-dependent fashion. Use of FIPC-1 in a quantitative chemoproteomics workflow reproducibly enriched protein targets in the thioredoxin, oxidoreductase, and protein disulfide isomerase (PDI) families, among others. In further interrogating the saturable targets of FIPC-1, we identified the PDI family member P4HB and the functionally uncharacterized protein NT5DC2, a member of the haloacid dehalogenase (HAD) superfamily, as previously unrecognized modulators of ferroptosis. Knockdown of these target genes sensitized cells to known ferroptosis inducers, while PACMA31, a previously reported inhibitor of P4HB, directly induced ferroptosis and was highly synergistic with erastin. Overall, this study introduces a new reactivity-based probe of the ferrous iron-dependent interactome and uncovers new targets for the therapeutic modulation of ferroptosis.



INTRODUCTION

Ferroptosis is an iron-dependent form of nonapoptotic cell death resulting from the accumulation of lipid hydroperoxides due to the loss or inhibition of the cellular machinery that make up a lipid peroxide defense network.^{1–4} Three key nodes of this network have been identified: the glutathione (GSH)-dependent lipid peroxidase GPX4,^{5–7} the cystine–glutamate antiporter system Xc[–],^{8–10} and most recently a GSH-independent pathway involving the lipophilic antioxidant coenzyme Q10 (CoQ10) and the CoQ oxidoreductase ferroptosis suppressor protein 1 (FSP1).^{11,12} Ferroptosis can be inhibited by iron chelators like desferoxamine (DFO) and small molecule antioxidants such as ferrostatin-1^{13,14} (Fer-1), which prevent lipid reactive oxygen species accumulation. Executioner caspases are not significantly activated in ferroptosis, and thus caspase inhibition does not protect cells from ferroptosis. Like apoptosis, however, ferroptosis is thought to serve a tumor-suppressive function,^{15,16} tipping oxidatively stressed cells toward death.

Ferroptosis has been implicated in various disease states, including neurodegeneration, ischemic organ injury, and cancer.³ A recent study¹⁷ revealed that CD8⁺ T cells, a classic

subtype of tumor-killing cells, drives ferroptosis in tumor cells, consistent with a tumor-suppressor function of the pathway, suggesting that its activation in certain tumors may have therapeutic potential. Moreover, so-called drug tolerant “persister” cells that survive targeted kinase inhibitor therapy and from which truly resistant tumor cells likely emerge were found to be highly reliant on GPX4 activity for survival and sensitive to ferroptosis.¹⁸ Thus, there is considerable interest in the potential of ferroptosis modulating small molecules as therapeutics.

Multiple classes of ferroptosis inducing small molecules have been described to date. Thus, erastin and sorafenib block cystine uptake through inhibition of the system Xc[–], while (1S,3R)-RSL3 and its analogues inactivate GPX4.² The small molecule FIN56 acts by depleting the GPX4 protein and

Received: June 22, 2020

simultaneously causing depletion of CoQ10.¹⁹ Perhaps most enigmatic among known ferroptosis inducers is FINO2 (Figure 1), a 1,2-dioxolane first described by Woerpel and co-

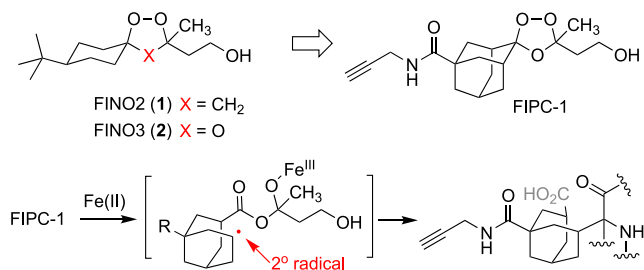


Figure 1. Structures of ferroptosis inducing peroxides FINO2 and FINO3 (top) and putative mechanism of FIPC-1 mediated protein labeling (bottom).

workers.²⁰ In a subsequent report exploring possible mechanism(s) of FINO2 action, the compound was found not to alter glutathione homeostasis, nor to inhibit GPX4 directly.²¹ FINO2 was shown to oxidize ferrous iron to the ferric state, consistent with a role for the peroxide bond in an initial Fenton-type reaction with labile ferrous iron. However, the endoperoxide function, while necessary, is not alone sufficient to induce ferroptosis. Thus, FINO2 analogues with seemingly minor structural modification, such as one carbon homologation of the hydroxy ethyl side chain, were without significant activity.²¹ This suggested to us that rather than conferring a generic peroxidic insult, FINO2 likely interacts with specific macromolecules, possibly including new, as yet unappreciated modulators of ferroptosis.

To explore this possibility, we designed and synthesized the probe FIPC-1 for Ferroptosis Inducing Peroxide for Chemo-proteomics 1 (Figure 1). Structurally, FIPC-1 is inspired by FINO2 but is further endowed with a protein cross-linking functionality borrowed from the well-studied antimalarial artemisinin.²² The adamantane-2,3'-[1,2,4]-trioxolane ring system present in FIPC-1 is known to react selectively with Fe²⁺ over other divalent metal ions, with initial O–O bond scission followed rapidly by β -scission to form a carbon-centered radical intermediate capable of protein cross-linking (Figure 1).²³ The Fe²⁺ promoted reactivity of 1,2-dioxolanes, by contrast, involves sequential one-electron reductions to afford diols,²⁴ making dioxolanes like FINO2 unlikely to undergo the cross-linking reactions desirable for chemo-proteomic applications (Figure S1). The conjoining in FIPC-1 of Fe²⁺ reactivity with protein labeling obviates the need for extra electrophilic or photoactivatable moieties; only the addition of an alkyne is required to enable subsequent visualization or capture of protein adducts for analysis.

Using analogues that bridge the structural differences between FINO2 and FIPC-1, we demonstrate that FIPC-1 both induces ferroptosis and forms protein adducts in an iron-dependent fashion, as expected. Using FIPC-1 in a quantitative chemoproteomics workflow, we observed reproducible enrichment of ~45 proteins, including multiple oxidoreductases and several proteins in the thioredoxin network, both protein families having been previously linked to ferroptosis.²⁵ Of greatest interest, however, were a small number of targets that showed “saturable” modification by FIPC-1 in competitive tandem-mass tag (TMT) labeling experiments. These included the oxidoreductases AKR1B1 and CBRI, two protein disulfide

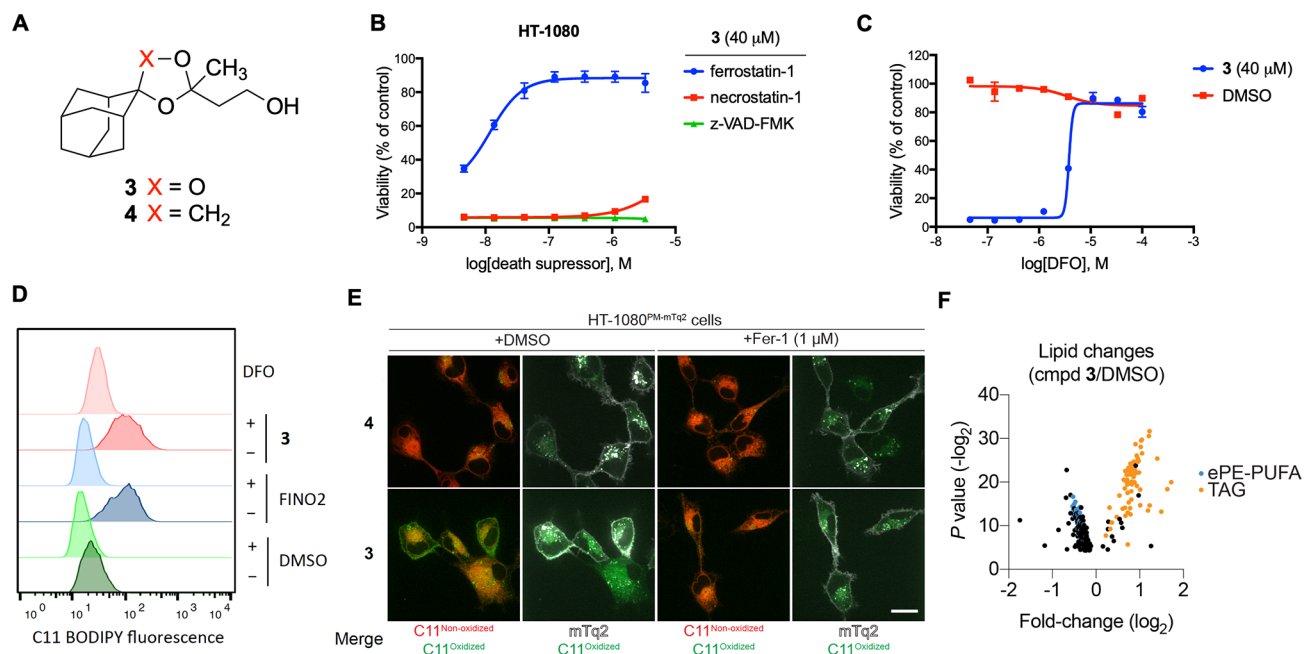


Figure 2. Trioxolane 3 is a peroxide-dependent inducer of ferroptosis. (A) Structures of 3 and nonperoxidic control 4. (B) Viability at 24 h of HT-1080 cells cotreated with 3 (40 μ M) and increasing concentrations of ferrostatin-1, necrostatin-1, or z-VAD-FMK. (C) Viability at 24 h of HT-1080 cells cotreated with a cytotoxic dose of 3 (40 μ M) or DMSO and increasing concentrations of the iron chelator DFO. (D) Lipid peroxidation in HT-1080 cells assessed by flow cytometry using C11 BODIPY after cells were incubated with vehicle (DMSO) or ferroptosis inducers (10 μ M) with or without DFO (50 μ M) for 5 h. (E) Compound 3 (20 μ M) but not control 4 induced lipid peroxidation as detected with C11 BODIPY 581/591 in HT-1080^{PM-mTq} cells expressing mTurquoise protein in plasma membrane (green). Ferrostatin-1 (1 μ M) prevented 3-induced lipid peroxidation. Scale bar = 20 μ m. (F) Lipids whose abundance was significantly altered in HT-1080 cells upon treatment for 5 h with 3. PUFA-containing phosphatidylethanolamine ether lipids (ePE) are colored blue and triacylglycerols (TAG) orange.

isomerases (PDIA6 and P4HB), the mitochondrial peroxidase PRDX3, and most intriguingly NT5DC2, a functionally uncharacterized member of the HAD superfamily of phosphatases. Genetic and pharmacological modulation of these targets identified P4HB and NT5DC2 as most closely linked to the ferroptotic phenotype; knockdown of either target sensitized cells to erastin and RSL3, while a known PDI inhibitor directly induced ferroptosis and synergized with erastin. Overall, our studies provide a new tool for chemoproteomic studies of the iron(II)-dependent interactome in live cells. As applied specifically to a ferroptosis sensitive cell type, FIPC-1 revealed new cellular modulators of ferroptosis and possible drug targets for therapeutic intervention in cancer and other disease states where the induction of ferroptosis is desirable.

RESULTS AND DISCUSSION

Previously reported structure–activity relationship (SAR) studies²¹ of FINO2 (**1**) defined the importance of the peroxide bond and hydroxyethyl side chain for ferroptosis induction. We explored the effect of replacing the 1,2-dioxolane with a 1,2,4-trioxolane ring, to afford “FINO3” (**2**), and then replaced the substituted cyclohexane ring of FINO2 with the adamantane ring that we predicted would enable protein cross-linking activity (compound **3**, Figure 2A). The 1,3-dioxolane **4**, a non-peroxidic control, was also synthesized, as was an analogue (**5**) in which the hydroxyethyl side chain of **3** is constrained as part of a cyclohexane ring (Figure S2). These analogues served as a structural and pharmacological bridge between FINO2 and FIPC-1, the latter being an analogue of **3** bearing an alkyne functionality for Cu(I)-catalyzed [3 + 2] azide–alkyne cycloaddition (CuAAC)-mediated coupling to fluorescent dyes or avidity (biotin) reagents.

We next assessed the cytotoxicity of the new peroxides versus FINO2 control in HT-1080 fibrosarcoma cells, a ferroptosis-sensitive cell line that is widely used in studies of the ferroptosis pathway. We found that FINO3 ($EC_{50} = 3.2 \mu\text{M}$) and **3** ($EC_{50} = 9.7 \mu\text{M}$) induced cell death at similar concentrations as FINO2 ($EC_{50} = 2.5 \mu\text{M}$) after 24 h treatment (Figure S2). Analogues **4** and **5** by contrast were essentially nontoxic in HT-1080 cells ($EC_{50} > 100 \mu\text{M}$), suggesting the importance of the peroxide function as well as the orientation of the hydroxyethyl side in delivering a cytotoxic insult.

To confirm that compounds **2** and **3** confer cell death via ferroptosis, HT-1080 cells were treated with a lethal concentration of FINO2, **2**, or **3**, along with increasing concentrations of one of three different death-suppressing compounds. We found that cell death induced by FINO2, **2**, and **3** was reversed by the antioxidant ferrostatin-1 but not by necroptosis or apoptosis inhibitors (Figure 2B and Figure S3). Cell death by the compounds could also be rescued with iron chelator DFO (Figure 2C and Figure S3B). This suggested that certain 1,2,4-trioxolanes, like the 1,2-dioxolane FINO2, can induce ferroptosis. Because compound **3** includes the antimalarial pharmacophore present in arterolane and artefenomel (Figure S4A), we also tested these compounds in HT-1080 cells. Exhibiting EC_{50} values similar to **3** in HT-1080 cells, coadministration of death-suppressing compounds indicated that arterolane, but not artefenomel, induces ferroptosis-like killing (Figure S4B,C). Taken together, these studies suggested that a peroxide function is necessary, but not

alone sufficient for ferroptosis induction by 1,2,4-trioxolanes, much as is also true for FINO2 and its analogues. Moreover, these studies confirmed that analogue **3**, on which FIPC-1 is based, is a bona fide inducer of ferroptosis.

To further validate that **3** induces lipid peroxidation, a defining event in ferroptosis,^{13,26} HT-1080 cells were treated with FINO2 or **3**, and the increase in fluorescence intensity of lipid peroxidation was evaluated with the lipid probe C11 BODIPY 581/591, as recorded by flow cytometry. Similar to FINO2, **3** produced a clear increase in lipid peroxidation and was suppressed by cotreatment with DFO (Figure 2D). In addition, **3**-induced lipid peroxidation occurred on internal membranes and at the plasma membrane as determined with whole-cell imaging of HT-1080^{PM-mTq} cells expressing plasma membrane-localized mTurquoise2²⁷ and could be inhibited by cotreatment with ferrostatin-1 (Figure 2E). No increase in lipid peroxidation was observed for the non-peroxide analogue **4** in the same experiment, indicating that the peroxide function in **3** is necessary for the observed phenotype. These data lend further support for the conclusion that compound **3** induces ferroptosis in HT-1080 cells.

We next explored the effects of compound **3** on global lipid abundance in HT-1080 cells. Consistent with previous observations of ferroptotic cells,²⁸ treatment with **3** resulted in significant depletion of numerous PUFA-containing phospholipids, notably including many PUFA-containing phosphatidylethanolamine ether lipids (ePEs) (Figure 2F, in blue). Compound **3** treatment also resulted in significant accumulation of diverse triacylglycerols, possibly because of inhibition of one or more mitochondrial proteins leading to disruption of β -oxidation and subsequent accumulation of free fatty acids that are stored in TAGs (Figure 2F, in orange). The full list of lipids analyzed are provided as a data set in the Supporting Information.

Finally, we assessed the possible effects of **3** on established regulators of ferroptosis. Whereas $2 \mu\text{M}$ of the system Xc^- inhibitor erastin2 effectively depleted total glutathione in A549 cells, treatment with **3** at a concentration ($40 \mu\text{M}$) that robustly induces ferroptosis had no significant effect on glutathione levels (Figure S5). We also compared the toxicities of RSL3 and **3** in A375 WT and GPX4 KO cell lines¹⁸ and found the cytotoxicity of RSL3 was significantly reduced in the GPX4 KO line, whereas compound **3** exhibited similar cell-killing effects whether or not GPX4 was present (Figure S5). This suggested that GPX4 is not a direct target of **3**. Finally, because susceptibility to ferroptosis has been associated with the RAS oncogene, we evaluated the selective lethality of erastin, RSL3, and **3** in inducible KRAS (G12D) AK210 cells cultured with or without doxycycline for 72 h to turn ON/OFF the KRAS (G12D) expression. We observed that cells expressing mutant KRAS were sensitized to erastin, RSL3, and **3** (Figure S6). Together these studies suggest compound **3**, like FINO2, induces ferroptosis by a mechanism distinct from the canonical ferroptosis inducers erastin and RSL3 and further implied that a chemoproteomic probe based on **3** (i.e., FIPC-1) could have utility in discerning as yet unappreciated modulators of ferroptosis.

Next we evaluated cell killing by FIPC-1 as well as its predicted ability to label proteins in an iron-dependent fashion. Although somewhat less potent than FINO2 or **3**, cell killing by FIPC-1 was reversed by DFO or ferrostatin-1, but not by necrostatin-1 or caspase inhibitor Z-VAD-FMK (Figure S7A,B), indicating that FIPC-1, like **3**, kills cells by ferroptosis.

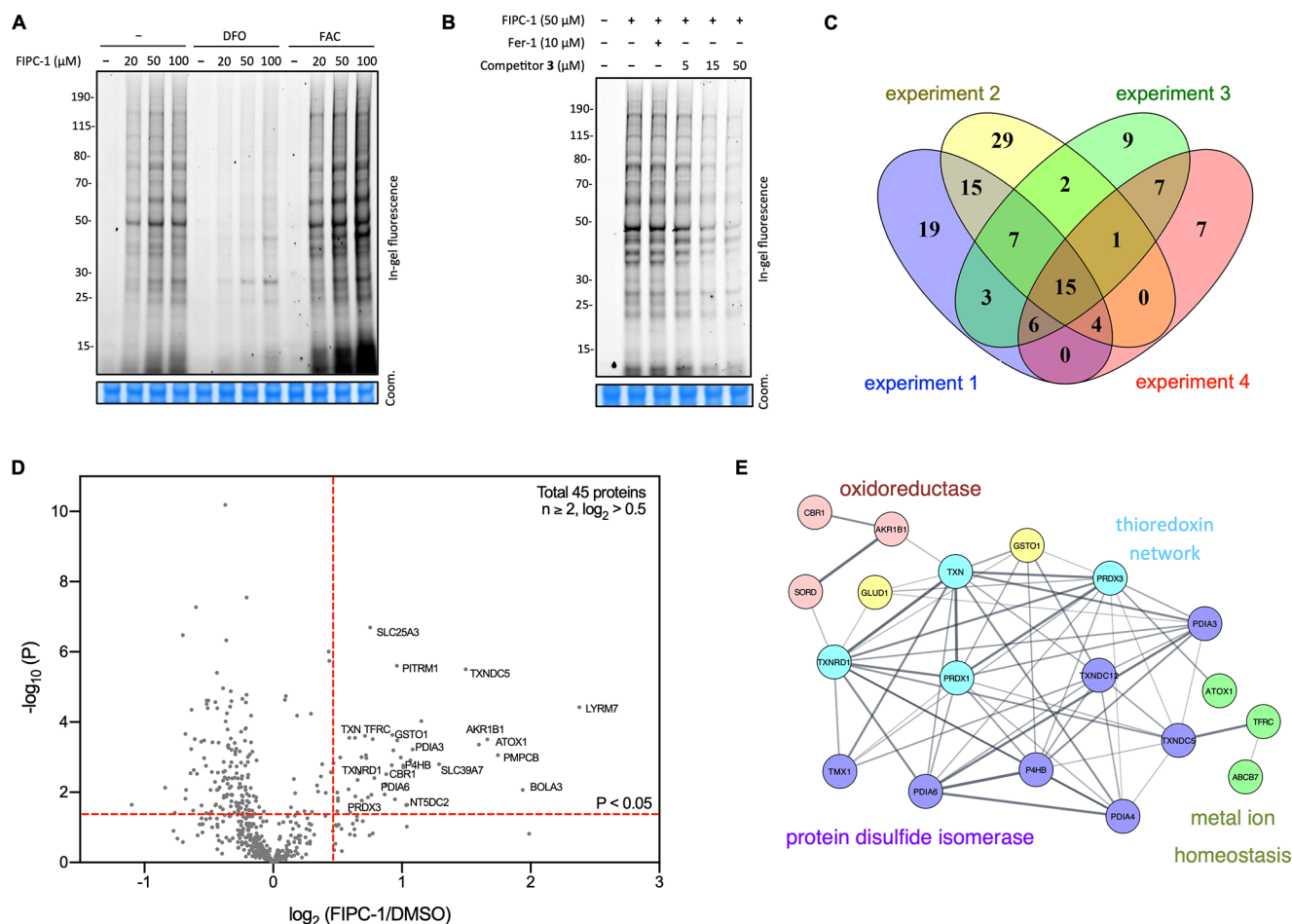


Figure 3. Cellular targets of FIPC-1 in HT-1080 cells. (A) Labeling of cellular proteins by FIPC-1 in HT-1080 cells is concentration- and iron-dependent (FAC = ferric ammonium citrate). Coomassie blue staining was used as a loading control. (B) Labeling by FIPC-1 is reduced in a dose-dependent fashion by pretreatment with compound 3 but not antioxidant ferrostatin-1. (C) Congruence of proteins enriched >1.4 -fold by FIPC-1 ($\log_2 > 0.5$) over DMSO control in four separate proteomic experiments. (D) Volcano plot of enriched FIPC-1 target proteins found in $n \geq 2$ experiments and enriched over DMSO control by fold change >1.4 ($\log_2 > 0.5$) and $P < 0.05$ in HT-1080 cells. (E) Interactome network highlighting 19 proteins enriched by FIPC-1 and known to be involved in redox processes. The complete network is provided as [Supporting Information](#).

To explore its protein cross-linking activity, cells were treated with FIPC-1 at 1, 10, 50, and 100 μM for 5 h or at 100 μM for between 2 and 8 h followed by cell lysis, CuAAC reaction with TAMRA-azide, separation by SDS-PAGE, and in-gel fluorescence scanning (Figure S7C,D). These studies revealed time- and concentration-dependent labeling of the HT-1080 proteome and identified a concentration–time regime optimal for further experimentation. Importantly, subsequent experiments in cells preconditioned with exogenous iron (as ferric ammonium citrate, FAC) or with DFO established that protein labeling by FIPC-1 is an iron-dependent process, as expected (Figure 3A). Although 1 μM ferrostatin-1 is sufficient to rescue cells from FIPC-1 induced ferroptosis (Figure S7B), a 10-fold higher concentration had no apparent effect on FIPC-1 labeling efficiency (Figure 3B). Importantly, labeling by FIPC-1 could be blocked with increasing concentrations of 3 as competitor (Figure 3B).

To identify the proteins that associate with FIPC-1 in an iron-dependent manner, we applied chemoproteomics with tandem mass tag (TMT) quantification. Hence, HT-1080 cells were treated with DMSO or FIPC-1 for 5 h, followed by cell lysis, CuAAC reaction with biotin-azide, enrichment with neutravidin beads, on-bead tryptic digestion, TMT labeling,

and combined analysis by LC-MS/MS analysis using TMT-based quantification. We compared lists of target proteins enriched >1.4 -fold by FIPC-1 over DMSO control in four separate labeling experiments and found reasonable congruence between experiments, including 15 protein targets enriched in all four experiments (Figure 3C). This was reassuring, given that a recent report²⁹ has questioned the reproducibility of earlier chemoproteomic studies^{30–32} involving cross-linking probes based on artemisinin and arterolane.

From the four data sets, a total of 45 proteins were found to be enriched compared to DMSO control in at least two experiments using an enrichment cutoff of fold change >1.4 ($\log_2 > 0.5$) and P value < 0.05 (Figure 3D). The use of a relatively low threshold for enrichment was employed to broadly assess the range of potential targets of FIPC-1, given its novel mode of activation/cross-linking as compared to established photoaffinity or cysteine-reactive modalities. Of the 45 targets identified by these enrichment criteria, many were involved in the regulation of cellular redox homeostasis, including members of the thioredoxin network, the protein disulfide isomerase (PDI) family, and NADPH-dependent oxidoreductases. The results of a Cytoscape with STRING^{33,34} analysis for this subset of the interactome is shown above

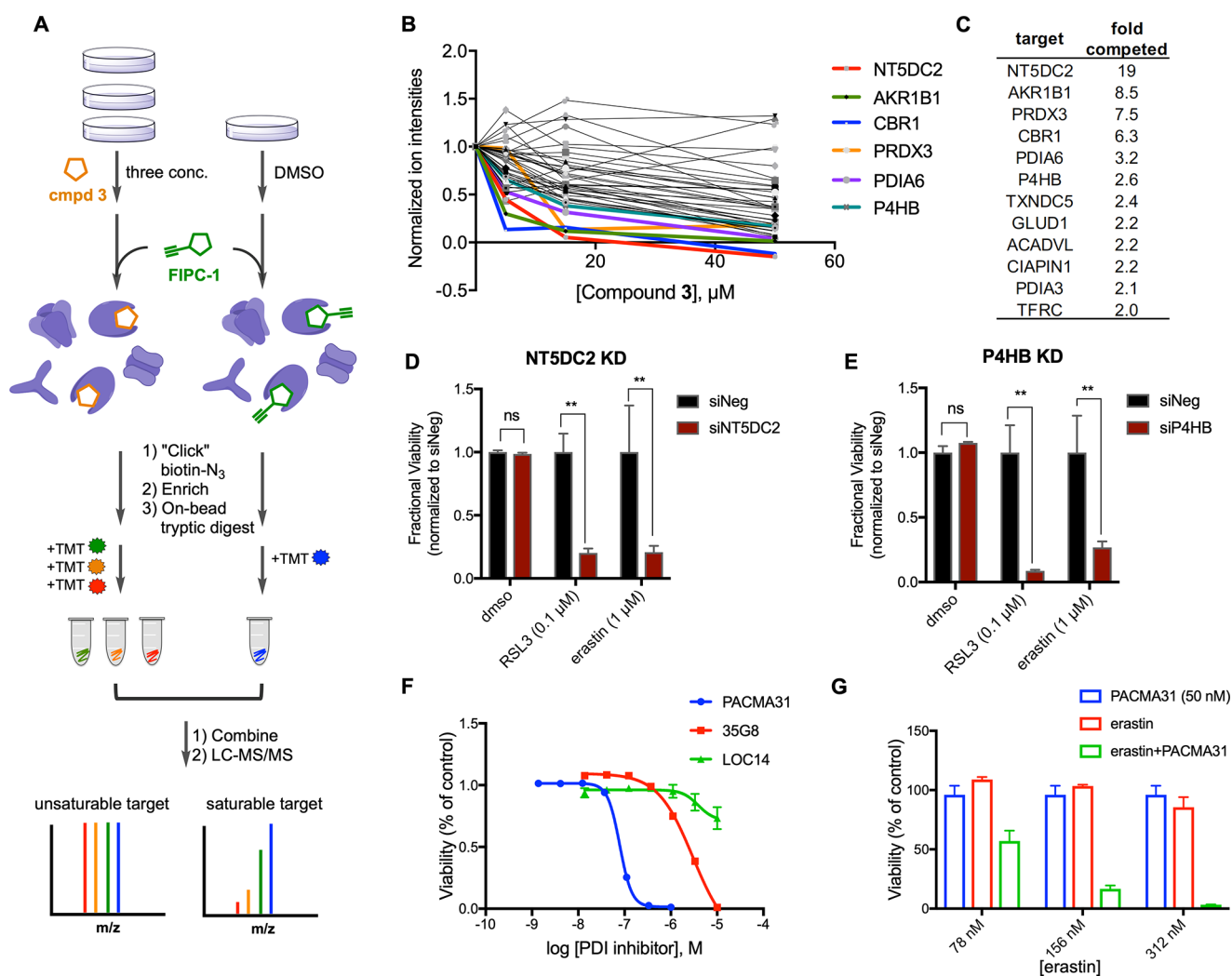


Figure 4. Quantitative chemoproteomics with FIPC-1 reveals saturable targets. (A) General workflow for chemoproteomics using FIPC-1 in the absence or presence of increasing concentrations (5, 15, or 50 μM) of competitor 3 and tandem mass tag mass spectrometry. (B) Saturable targets exhibit a dose-dependent decrease in FIPC-1 labeling with increasing concentrations of competitor 3. (C) List of partially competed protein targets of FIPC-1 (from experiment with 15 μM competitor 3). (D) siRNA knockdown of NT5DC2 sensitized HT-1080 cells to RSL3 and erastin. (E) siRNA knockdown of P4HB rendered HT-1080 cells hypersensitive to RSL3 and erastin. (F) Cell viability at 24 h of HT-1080 cells treated with reported PDI inhibitors 35G8, PACMA31 and LOC14. (G) Cell killing by PACMA31 (at 50 nM) and erastin at three concentrations alone or combined (green); viability of HT-1080 cells at 24 h of incubation. In (D, E), data are plotted as mean \pm s.e.m. with $n \geq 3$ biological replicates. 2way ANOVA multiple comparisons; **** $P \leq 0.0001$, *** $P \leq 0.001$, ** $P \leq 0.01$, * $P \leq 0.05$, ns $P > 0.5$.

(Figure 3E), and the complete list of enriched targets is provided in the Supporting Information (Figure S8). Notably, a very small number of iron-binding or utilizing proteins were among the enriched protein targets. This was consistent with the expectation that FIPC-1 should be activated by an unbound, labile ferrous iron, but not by the large number of cellular proteins that utilize iron cofactors. The latter forms of iron are tightly bound in enzyme active sites and generally should not be accessible sterically for reaction with the hindered peroxide in FIPC-1.

We next performed competitive labeling to discern saturable targets from high abundance proteins that might be enriched through nonspecific labeling. In this experiment (Figure 4A), HT-1080 cells were pretreated with DMSO or three different concentrations (5, 15, or 50 μM) of 3 as a competitor for iron-dependent interaction, followed 0.25 h later by the addition of 50 μM FIPC-1, and the same TMT/MS workflow described above. Gratifyingly, the majority of enriched target proteins

showed at least partially saturable labeling (Figure 4B). Among the most robustly competed targets were 5'-nucleotidase domain-containing protein 2 (NT5DC2), aldose reductase (AKR1B1), proxiredoxin-3 (PRDX3), and carbonyl reductase (CBR1), all of which were >80% competed at 15 μM of competitor 3 (Figure 4B). Targets competed >50% by 15 μM 3 included four members of the protein disulfide isomerase family: protein disulfide isomerase A6 (PDIA6), protein disulfide isomerase (P4HB), thioredoxin domain containing 5 (TXNDC5), and protein disulfide isomerase A3 (PDIA3); glutamate dehydrogenase 1 (GLUD1); transferrin receptor protein 1 (TFRC); very long chain acyl-CoA dehydrogenase (ACADVL); and iron-sulfur cluster assembly protein (CIAPIN1) (Figure 4C). Certain targets like thioredoxin (TXN) and thioredoxin reductase (TXNRD1), though moderately enriched in the pull-down experiment, were not competed by 3. It seems plausible that the enrichment of these proteins may reflect their overall upregulation in response to 3

or FIPC-1. Thus, the competition experiment in this case serves to distinguish saturable targets of FIPC-1 from apparent “enrichment” (false positives) arising from a cellular response to the xenobiotic peroxide molecule itself.

Having identified several members of a FIPC-1 iron-dependent interactome, we next considered their known biological activities and possible roles in ferroptosis. AKR1B1 encodes an aldose reductase, a member of the family that converts glucose to sorbitol during hyperglycemia but is also capable of reducing toxic aldehyde byproducts of lipid peroxidation, namely 4-hydroxy-*trans*-2-nonenal (4-HNE) and its glutathione adducts, to the corresponding alcohols.^{35,36} Similarly, the carbonyl reductase encoded by CBR1 counts among known substrates 4-HNE as well as prostaglandins and the quinones tocopherolquinone (vitamin E) and ubiquinone-1 (coenzyme Q1).^{37,38} Thus, a protective role for AKR1B1 and CBR1 in the later stages of ferroptosis can be readily envisioned. Of note is that AKR1C1, a close family member to AKR1B1, was found previously to be upregulated in erastin-resistant cells.⁸ The mitochondria localized PRDX3 is a peroxidase that catalyzes the reduction of hydrogen peroxide, limiting availability of this species for Fenton reaction and hydroxy radical generation.³⁹ Finally, four members of the protein disulfide isomerase (PDI) family were identified in the FIPC-1 iron-dependent interactome. The PDIs are multifunctional endoplasmic reticulum (ER) enzymes that mediate disulfide formation and protein folding.⁴⁰

We performed knockdown of individual target genes in HT-1080 cells using siRNA pools targeting the specific genes. Despite achieving over 95% knockdown of mRNA levels, we observed only moderate impairment of cell growth with knockdown of CBR1, AKR1B1, or PRDX3 (Figure S9A,B). We also evaluated the effects of AKR1B1 inhibitors developed for other clinic indication but found that none could alone trigger ferroptotic cell death in HT-1080 cells (Figure S9C). Given that 4-HNE should be elevated during GPX4 inhibition, we looked for synergy between GPX4 inhibition and AKR1B1 or CBR1 knockdown (Figure S10). We found that knockdown of CBR1, AKR1B1, or PRDX3 did not additionally sensitize HT-1080 cells to RSL3 or indeed to any of the canonical ferroptosis inducers studied, including 3 (Figure S10). Paradoxically, knockdown of CBR1 or AKR1B1 protected HT-1080 cells from erastin toxicity, an observation that might be explained by a compensatory antioxidant response to the KD of these genes, a possibility that merits further study.

The most robustly (~19-fold) competed protein in the FIPC-1 screen was the protein NT5DC2. Annotated as a mitochondrial localized member of the haloacid dehalogenase (HAD) superfamily,⁴¹ the functional activity and physiological relevance of this protein remain uncharacterized. Intriguingly then, siRNA knockdown of NT5DC2 significantly sensitized HT-1080 cells to both RSL3 and erastin (Figure 4D and Figure S10). In what is apparently the only previous report on this protein, NT5DC2 was proposed to associate with and stabilize Fyn (a proto-oncogene protein tyrosine kinase) to promote tumor progression in glioma stem-like cells.⁴² Because the HAD superfamily primarily comprises phosphatases, further study of NT5DC2 function, its interaction with Fyn kinase, and its larger role in the ferroptosis pathway is warranted.

Next we evaluated the effect of siRNA knockdown of four members of the protein disulfide isomerase family identified in the FIPC-1 interactome screen, namely PDIA6, P4HB,

TXNDC5, and PDIA3. Knockdown of individual PDIs in the absence of ferroptosis inducer had no effect on proliferation of HT-1080 cells. However, P4HB knockdown sensitized cells dramatically to RSL3 and erastin, but interestingly not to FINO2 or 3 (Figure 4E and Figure S11A). If labeling by FIPC-1 or 3 promoted PDI dysfunction in the ER, this might be expected to induce the unfolded protein response (UPR). To explore this possibility, we treated HT-1080 cells with compound 3 or a positive control inducer of the UPR, thapsigargin, and looked for induction of the UPR effector ATF4. Indeed, compound 3, like thapsigargin, led to ATF4 accumulation in HT-1080 cells (Figure S12A–C). Whether UPR induction by 3 is due solely or even primarily to interaction with PDIs cannot be discerned from these initial experiments but is nevertheless consistent with an underexplored connection⁸ between ferroptosis and the UPR.

Since several inhibitors of P4HB have been described in the literature, we next evaluated the effects of three such compounds in HT-1080 cells, alone and in combination with known ferroptosis inducers. Previously reported as PDI inhibitors, both PACMA31⁴³ and 35G8⁴⁴ (a 3-methyltoxoflavin) were indeed cytotoxic to HT-1080 cells, while the compound LOC14⁴⁵ was much less so (Figure 4F). To determine whether these compounds promote ferroptotic cell death specifically, we performed coincubations with death suppressing compounds as before. Notably, PACMA31 toxicity was mitigated or reversed by DFO and ferrostatin-1 but not other death suppressors, consistent with a mechanism of ferroptosis induction (Figure S13A–C). In contrast, 35G8-mediated cell death could not be rescued by any of the death suppressors, suggesting a different mechanism of action (Figure S13A). In fact, redox cycling toxoflavins, of which 35G8 is an example, are known to catalyze the conversion of oxygen to hydrogen peroxide⁴⁶ and interfere in enzymatic assays broadly, but especially perniciously in the case of cysteine/GSH dependent enzymes such as PDIs. The reported mechanism of PACMA31 action is more specific, namely, covalent binding to the catalytic cysteine in PDIs. That this compound, or PDI inhibition in general, can trigger ferroptosis has not to our knowledge been previously recognized. Because knockdown of P4HB alone failed to induce ferroptosis, the contribution of additional PDIs or other off-targets in the action of PACMA31 appears likely. In fact, PACMA31 was reported⁴⁷ to also inhibit PDI family members PDIA6 and PDIA3, both of which were among the protein targets identified with FIPC-1. While acknowledging the potential for cross-reactivity of PACMA31 even outside the PDI family, we note that widely used GPX4 inhibitors such as ML210 and RSL3 also possess cysteine reactive warheads and other structural similarities with PACMA31. Thus, the possibility that these well-established tool compounds may have additional targets cannot be formally excluded.

To further explore the potential utility of PACMA31 as a ferroptosis inducer, we next asked whether the compound exhibited synergy with canonical ferroptosis inducers erastin and RSL3. Indeed, we found that noncytotoxic concentrations of PACMA31 and erastin, when combined, produced a profound killing effect in HT-1080 cells (Figure 4G). By comparison, the combined effect of PACMA31 and RSL3 was only additive in nature (Figure S13D). An inhibitor of cysteine import, erastin rapidly depletes the cell of an essential cofactor (GSH) required for PDI function.⁴⁸ In this way, the dramatic synergy of system Xc⁻ and PDI inhibition revealed herein can

be understood and also suggests a potential therapeutic combination to target ferroptosis-sensitive cells selectively.

CONCLUSIONS

Here we describe FIPC-1, a new tool for chemoproteomic studies of the cellular ferrous iron-dependent interactome. Related structurally to ferroptosis inducing peroxides with predicted pleiotropic action, we hypothesized that FIPC-1 could identify new modulators of ferroptosis, including ancillary players that might be missed in single-gene screening approaches. Consistent with this, knockdown of individual FIPC-1 target genes did not sensitize HT-1080 cells to 3 yet did synergize with known ferroptosis inducers erastin and RSL3 (Figure S10). Iron-dependent and competitive protein labeling by FIPC-1 was demonstrated in a quantitative chemoproteomic workflow that identified several saturable protein targets, including P4HB and NT5DC2. A previously described inhibitor of P4HB was shown to directly induce ferroptosis and to synergize with system Xc⁻ inhibition, suggesting a potential therapeutic approach to selectively target mutant-RAS driven cancers. Finally, an important role in ferroptosis was uncovered for the uncharacterized HAD family member NT5DC2, suggesting an unexpected new avenue in the cellular machinery modulating ferroptosis. More broadly, FIPC-1 and related probes based on the same design principles are likely to find further utility in the study of diverse cellular processes mediated or impacted by the cytosolic ferrous iron pool.

ASSOCIATED CONTENT

Supporting Information

The Supporting Information is available free of charge at <https://pubs.acs.org/doi/10.1021/jacs.0c06709>.

Experimental details; Figures S1–S13 and Schemes S1–S4 (PDF)

Full list of lipids analyzed (XLSX)

Complete list of enriched targets (XLSX)

AUTHOR INFORMATION

Corresponding Author

Adam R. Renslo – Department of Pharmaceutical Chemistry, University of California, San Francisco, San Francisco, California 94143, United States; orcid.org/0000-0002-1240-2846; Email: adam.renslo@ucsf.edu

Authors

Ying-Chu Chen – Department of Pharmaceutical Chemistry, University of California, San Francisco, San Francisco, California 94143, United States

Juan A. Osés-Prieto – Department of Pharmaceutical Chemistry, University of California, San Francisco, San Francisco, California 94143, United States

Lauren E. Pope – Department of Biology, Stanford University, Stanford, California 94305, United States

Alma L. Burlingame – Department of Pharmaceutical Chemistry, University of California, San Francisco, San Francisco, California 94143, United States

Scott J. Dixon – Department of Biology, Stanford University, Stanford, California 94305, United States; orcid.org/0000-0001-6230-8199

Complete contact information is available at: <https://pubs.acs.org/doi/10.1021/jacs.0c06709>

Notes

The authors declare the following competing financial interest(s): S.J.D. is on the scientific advisory board of Ferro Therapeutics Inc., has consulted for Toray Industries and AbbVie Inc., and is an inventor on patents related to ferroptosis. A.R.R. is an advisor and co-founder of Theras, Inc., Elgia Therapeutics, and Tataro Therapeutics.

ACKNOWLEDGMENTS

S.J.D. acknowledges funding from the National Institutes of Health Research grant 1R01GM122923. A.R.R. acknowledges funding from National Institutes of Health grant R01AI105106 and Congressionally Directed Medical Research Program, grants W81XWH1810763 and W81XWH1810754. Mass spectrometry was provided by the Mass Spectrometry Resource at UCSF (A. L. Burlingame, Director) supported by the Dr. Miriam and Sheldon G. Adelson Medical Research Foundation (AMRF) and the UCSF Program for Breakthrough Biomedical Research (PBBR). We thank F. McCormick and E. Collisson (UCSF) for providing GPX4 KO A375 cells and R. Perera (UCSF) for the inducible KRAS (G12D) AK210 cells. We thank D. Medina-Cleghorn for experimental advice and L. Magtanong for help with imaging experiments. We acknowledge B. Blank and P. Talukder for synthesizing arterolane and artefenomel.

REFERENCES

- (1) Yu, H.; Guo, P.; Xie, X.; Wang, Y.; Chen, G. Ferroptosis, a New Form of Cell Death, and Its Relationships with Tumorous Diseases. *J. Cell Mol. Med.* **2017**, *21*, 648–657.
- (2) Yang, W. S.; Stockwell, B. R. Ferroptosis: Death by Lipid Peroxidation. *Trends Cell Biol.* **2016**, *26*, 165–176.
- (3) Stockwell, B. R.; Friedmann Angeli, J. P.; Bayir, H.; Bush, A. L.; Conrad, M.; Dixon, S. J.; Fulda, S.; Gascón, S.; Hatzios, S. K.; Kagan, V. E.; Noel, K.; Jiang, X.; Linkermann, A.; Murphy, M. E.; Overholtzer, M.; Oyagi, A.; Pagnussat, G. C.; Park, J.; Ran, Q.; Rosenfeld, C. S.; Salnikow, K.; Tang, D.; Torti, F. M.; Torti, S. V.; Toyokuni, S.; Woerpel, K. A.; Zhang, D. D. Ferroptosis: A Regulated Cell Death Nexus Linking Metabolism, Redox Biology, and Disease. *Cell* **2017**, *171*, 273–285.
- (4) Dixon, S. J.; Lemberg, K. M.; Lamprecht, M. R.; Skouta, R.; Zaitsev, E. M.; Gleason, C. E.; Patel, D. N.; Bauer, A. J.; Cantley, A. M.; Yang, W. S.; Morrison, B.; Stockwell, B. R. Ferroptosis: An Iron-Dependent Form of Nonapoptotic Cell Death. *Cell* **2012**, *149*, 1060–1072.
- (5) Yang, W. S.; SriRamaratnam, R.; Welsch, M. E.; Shimada, K.; Skouta, R.; Viswanathan, V. S.; Cheah, J. H.; Clemons, P. A.; Shamji, A. F.; Clish, C. B.; Brown, L. M.; Girotti, A. W.; Cornish, V. W.; Schreiber, S. L.; Stockwell, B. R. Regulation of Ferroptotic Cancer Cell Death by GPX4. *Cell* **2014**, *156*, 317–331.
- (6) Friedmann Angeli, J. P.; Schneider, M.; Proneth, B.; Tyurina, Y. Y.; Tyurin, V. A.; Hammond, V. J.; Herbach, N.; Aichler, M.; Walch, A.; Eggenhofer, E.; Basavarajappa, D.; Rådmark, O.; Kobayashi, S.; Seibt, T.; Beck, H.; Neff, F.; Esposito, I.; Wanke, R.; Förster, H.; Yefremova, O.; Heinrichmeyer, M.; Bornkamm, G. W.; Geissler, E. K.; Thomas, S. B.; Stockwell, B. R.; O'Donnell, V. B.; Kagan, V. E.; Schick, J. A.; Conrad, M. Inactivation of the Ferroptosis Regulator Gpx4 Triggers Acute Renal Failure in Mice. *Nat. Cell Biol.* **2014**, *16*, 1180–1191.
- (7) Conrad, M.; Friedmann Angeli, J. P. Glutathione Peroxidase 4 (Gpx4) and Ferroptosis: What's so Special about It? *Molecular & Cellular Oncology* **2015**, *2*, No. e995047.
- (8) Dixon, S. J.; Patel, D. N.; Welsch, M.; Skouta, R.; Lee, E. D.; Hayano, M.; Thomas, A. G.; Gleason, C. E.; Tatonetti, N. P.; Slusher, B. S.; Stockwell, B. R. Pharmacological Inhibition of Cystine-

Glutamate Exchange Induces Endoplasmic Reticulum Stress and Ferroptosis. *eLife* **2014**, *3*, No. e02523.

(9) Daher, B.; Parks, S. K.; Durivault, J.; Cormerais, Y.; Baidarjad, H.; Tambutte, E.; Pouysségur, J.; Vučićić, M. Genetic Ablation of the Cystine Transporter XCT in PDAC Cells Inhibits MTORC1, Growth, Survival, and Tumor Formation via Nutrient and Oxidative Stresses. *Cancer Res.* **2019**, *79*, 3877–3890.

(10) Badgley, M. A.; Kremer, D. M.; Maurer, H. C.; DelGiorno, K. E.; Lee, H.-J.; Purohit, V.; Sagalovskiy, I. R.; Ma, A.; Kapilian, J.; Firl, C. E. M.; Decker, A. R.; Sastra, S. A.; Palermo, C. F.; Andrade, L. R.; Sajjakulnukit, P.; Zhang, L.; Tolstyka, Z. P.; Hirschhorn, T.; Lamb, C.; Liu, T.; Gu, W.; Seeley, E. S.; Stone, E.; Georgiou, G.; Manor, U.; Iuga, A.; Wahl, G. M.; Stockwell, B. R.; Lyssiotis, C. A.; Olive, K. P. Cysteine Depletion Induces Pancreatic Tumor Ferroptosis in Mice. *Science* **2020**, *368*, 85–89.

(11) Bersuker, K.; Hendricks, J. M.; Li, Z.; Magtanong, L.; Ford, B.; Tang, P. H.; Roberts, M. A.; Tong, B.; Maimone, T. J.; Zoncu, R.; Bassik, M. C.; Nomura, D. K.; Dixon, S. J.; Olzmann, J. A. The CoQ Oxidoreductase FSP1 Acts Parallel to GPX4 to Inhibit Ferroptosis. *Nature* **2019**, *575*, 688–692.

(12) Doll, S.; Freitas, F. P.; Shah, R.; Aldrovandi, M.; da Silva, M. C.; Ingold, I.; Grocin, A. G.; Xavier da Silva, T. N.; Panzilius, E.; Scheel, C. H.; Mourão, A.; Buday, K.; Sato, M.; Wanninger, J.; Vignane, T.; Mohana, V.; Rehberg, M.; Flatley, A.; Schepers, A.; Kurz, A.; White, D.; Sauer, M.; Sattler, M.; Tate, E. W.; Schmitz, W.; Schulze, A.; O'Donnell, V.; Proneth, B.; Popowicz, G. M.; Pratt, D. A.; Angeli, J. P. F.; Conrad, M. FSP1 Is a Glutathione-Independent Ferroptosis Suppressor. *Nature* **2019**, *575*, 693–698.

(13) Zilka, O.; Shah, R.; Li, B.; Friedmann Angeli, J. P.; Griesser, M.; Conrad, M.; Pratt, D. A. On the Mechanism of Cytoprotection by Ferrostatin-1 and Liproxstatin-1 and the Role of Lipid Peroxidation in Ferroptotic Cell Death. *ACS Cent. Sci.* **2017**, *3*, 232–243.

(14) Skouta, R.; Dixon, S. J.; Wang, J.; Dunn, D. E.; Orman, M.; Shimada, K.; Rosenberg, P. A.; Lo, D. C.; Weinberg, J. M.; Linkermann, A.; Stockwell, B. R. Ferrostatins Inhibit Oxidative Lipid Damage and Cell Death in Diverse Disease Models. *J. Am. Chem. Soc.* **2014**, *136*, 4551–4556.

(15) Stockwell, B. R.; Jiang, X. A. Physiological Function for Ferroptosis in Tumor Suppression by the Immune System. *Cell Metab.* **2019**, *30*, 14–15.

(16) Ubellacker, J. M.; Tasdogan, A.; Ramesh, V.; Shen, B.; Mitchell, E. C.; Martin-Sandoval, M. S.; Gu, Z.; McCormick, M. L.; Durham, A. B.; Spitz, D. R.; Zhao, Z.; Mathews, T. P.; Morrison, S. J. Lymph Protects Metastasizing Melanoma Cells from Ferroptosis. *Nature* **2020**, *585*, 113.

(17) Wang, W.; Green, M.; Choi, J. E.; Gijón, M.; Kennedy, P. D.; Johnson, J. K.; Liao, P.; Lang, X.; Kryczek, I.; Sell, A.; Xia, H.; Zhou, J.; Li, G.; Li, J.; Li, W.; Wei, S.; Vatan, L.; Zhang, H.; Szeliga, W.; Gu, W.; Liu, R.; Lawrence, T. S.; Lamb, C.; Tanno, Y.; Cieslik, M.; Stone, E.; Georgiou, G.; Chan, T. A.; Chinnaiyan, A.; Zou, W. CD8+ T Cells Regulate Tumour Ferroptosis during Cancer Immunotherapy. *Nature* **2019**, *569*, 270–274.

(18) Hangauer, M. J.; Viswanathan, V. S.; Ryan, M. J.; Bole, D.; Eaton, J. K.; Matov, A.; Galeas, J.; Dhruv, H. D.; Berens, M. E.; Schreiber, S. L.; McCormick, F.; McManus, M. T. Drug-Tolerant Persister Cancer Cells Are Vulnerable to GPX4 Inhibition. *Nature* **2017**, *551*, 247–250.

(19) Shimada, K.; Skouta, R.; Kaplan, A.; Yang, W. S.; Hayano, M.; Dixon, S. J.; Brown, L. M.; Valenzuela, C. A.; Wolpaw, A. J.; Stockwell, B. R. Global Survey of Cell Death Mechanisms Reveals Metabolic Regulation of Ferroptosis. *Nat. Chem. Biol.* **2016**, *12*, 497–503.

(20) Abrams, R. P.; Carroll, W. L.; Woerpel, K. A. Five-Membered Ring Peroxide Selectively Initiates Ferroptosis in Cancer Cells. *ACS Chem. Biol.* **2016**, *11*, 1305–1312.

(21) Gaschler, M. M.; Andia, A. A.; Liu, H.; Csuka, J. M.; Hurlocker, B.; Vaiana, C. A.; Heindel, D. W.; Zuckerman, D. S.; Bos, P. H.; Reznik, E.; Ye, L. F.; Tyurina, Y. Y.; Lin, A. J.; Shchepinov, M. S.; Chan, A. Y.; Peguero-Pereira, E.; Fomich, M. A.; Daniels, J. D.;

Bekish, A. V.; Shmanai, V. V.; Kagan, V. E.; Mahal, L. K.; Woerpel, K. A.; Stockwell, B. R. FINO2 Initiates Ferroptosis through GPX4 Inactivation and Iron Oxidation. *Nat. Chem. Biol.* **2018**, *14*, 507–515.

(22) Vennerstrom, J. L.; Arbe-Barnes, S.; Brun, R.; Charman, S. A.; Chiu, F. C. K.; Chollet, J.; Dong, Y.; Dorn, A.; Hunziker, D.; Matile, H.; McIntosh, K.; Padmanilayam, M.; Santo Tomas, J.; Scheurer, C.; Scorneaux, B.; Tang, Y.; Urwyler, H.; Wittlin, S.; Charman, W. N. Identification of an Antimalarial Synthetic Trioxolane Drug Development Candidate. *Nature* **2004**, *430*, 900–904.

(23) Tang, Y.; Dong, Y.; Wang, X.; Sriraghavan, K.; Wood, J. K.; Vennerstrom, J. L. Dispiro-1,2,4-Trioxane Analogues of a Prototype Dispiro-1,2,4-Trioxolane: Mechanistic Comparators for Artemisinin in the Context of Reaction Pathways with Iron(II). *J. Org. Chem.* **2005**, *70*, 5103–5110.

(24) Wang, X.; Dong, Y.; Wittlin, S.; Creek, D.; Chollet, J.; Charman, S. A.; Tomas, J. S.; Scheurer, C.; Snyder, C.; Vennerstrom, J. L. Spiro- and Dispiro-1,2-Dioxolanes: Contribution of Iron(II)-Mediated One-Electron vs Two-Electron Reduction to the Activity of Antimalarial Peroxides. *J. Med. Chem.* **2007**, *50*, 5840–5847.

(25) Llabani, E.; Hicklin, R. W.; Lee, H. Y.; Motika, S. E.; Crawford, L. A.; Weerapana, E.; Hergenrother, P. J. Diverse Compounds from Pleuromutilin Lead to a Thioredoxin Inhibitor and Inducer of Ferroptosis. *Nat. Chem.* **2019**, *11*, 521–532.

(26) Yang, W. S.; Kim, K. J.; Gaschler, M. M.; Patel, M.; Shchepinov, M. S.; Stockwell, B. R. Peroxidation of Polyunsaturated Fatty Acids by Lipoxygenases Drives Ferroptosis. *Proc. Natl. Acad. Sci. U. S. A.* **2016**, *113*, E4966–75.

(27) Magtanong, L.; Ko, P.-J.; To, M.; Cao, J. Y.; Forcina, G. C.; Tarangelo, A.; Ward, C. C.; Cho, K.; Patti, G. J.; Nomura, D. K.; Olzmann, J. A.; Dixon, S. J. Exogenous Monounsaturated Fatty Acids Promote a Ferroptosis-Resistant Cell State. *Cell Chem. Biol.* **2019**, *26*, 420–432.

(28) Kagan, V. E.; Mao, G.; Qu, F.; Angeli, J. P. F.; Doll, S.; Croix, C. S.; Dar, H. H.; Liu, B.; Tyurin, V. A.; Ritov, V. B.; Kapralov, A. A.; Amoscato, A. A.; Jiang, J.; Anthonymuthu, T.; Mohammadyani, D.; Yang, Q.; Proneth, B.; Klein-Seetharaman, J.; Watkins, S.; Bahar, I.; Greenberger, J.; Mallampalli, R. K.; Stockwell, B. R.; Tyurina, Y. Y.; Conrad, M.; Bayır, H. Oxidized Arachidonic and Adrenic PES Navigate Cells to Ferroptosis. *Nat. Chem. Biol.* **2017**, *13*, 81–90.

(29) Jourdan, J.; Walz, A.; Matile, H.; Schmidt, A.; Wu, J.; Wang, X.; Dong, Y.; Vennerstrom, J. L.; Schmidt, R. S.; Wittlin, S.; Mäser, P. Stochastic Protein Alkylation by Antimalarial Peroxides. *ACS Infect. Dis.* **2019**, *5*, 2067–2075.

(30) Ismail, H. M.; Barton, V.; Panchana, M.; Charoensutthivarakul, S.; Wong, M. H. L.; Hemingway, J.; Biagini, G. A.; O'Neill, P. M.; Ward, S. A. Artemisinin Activity-Based Probes Identify Multiple Molecular Targets within the Asexual Stage of the Malaria Parasite *Plasmodium falciparum* 3D7. *Proc. Natl. Acad. Sci. U. S. A.* **2016**, *113*, 2080–2085.

(31) Ismail, H. M.; Barton, V. E.; Panchana, M.; Charoensutthivarakul, S.; Biagini, G. A.; Ward, S. A.; O'Neill, P. M. A Click Chemistry-Based Proteomic Approach Reveals That 1,2,4-Trioxolane and Artemisinin Antimalarials Share a Common Protein Alkylation Profile. *Angew. Chem., Int. Ed.* **2016**, *55*, 6401–6405.

(32) Wang, J.; Zhang, C.-J.; Chia, W. N.; Loh, C. C. Y.; Li, Z.; Lee, Y. M.; He, Y.; Yuan, L.-X.; Lim, T. K.; Liu, M.; Liew, C. X.; Lee, Y. Q.; Zhang, J.; Lu, N.; Lim, C. T.; Hua, Z.-C.; Liu, B.; Shen, H.-M.; Tan, K. S. W.; Lin, Q. Haem-Activated Promiscuous Targeting of Artemisinin in *Plasmodium falciparum*. *Nat. Commun.* **2015**, *6*, 10111.

(33) Szklarczyk, D.; Gable, A. L.; Lyon, D.; Junge, A.; Wyder, S.; Huerta-Cepas, J.; Simonovic, M.; Doncheva, N. T.; Morris, J. H.; Bork, P.; Jensen, L. J.; Von Mering, C. STRING V11: Protein-Protein Association Networks with Increased Coverage, Supporting Functional Discovery in Genome-Wide Experimental Datasets. *Nucleic Acids Res.* **2019**, *47*, D607–D613.

(34) Doncheva, N. T.; Morris, J. H.; Gorodkin, J.; Jensen, L. J. Cytoscape Stringapp: Network Analysis and Visualization of Proteomics Data. *J. Proteome Res.* **2019**, *18*, 623–632.

(35) Maccari, R.; Ottanà, R. Targeting Aldose Reductase for the Treatment of Diabetes Complications and Inflammatory Diseases: New Insights and Future Directions. *J. Med. Chem.* **2015**, *58*, 2047–2067.

(36) Srivastava, S.; Dixit, B. L.; Cai, J.; Sharma, S.; Hurst, H. E.; Bhatnagar, A.; Srivastava, S. K. Metabolism of Lipid Peroxidation Product, 4-Hydroxynonenal (HNE) in Rat Erythrocytes: Role of Aldose Reductase. *Free Radical Biol. Med.* **2000**, *29*, 642–651.

(37) Wermuth, B. Purification and Properties of an NADPH-Dependent Carbonyl Reductase from Human Brain. Relationship to Prostaglandin 9-Ketoreductase and Xenobiotic Ketone Reductase. *J. Biol. Chem.* **1981**, *256*, 1206–1213.

(38) Rotondo, R.; Moschini, R.; Renzone, G.; Tuccinardi, T.; Balestri, F.; Cappiello, M.; Scaloni, A.; Mura, U.; Del-Corso, A. Human Carbonyl Reductase 1 as Efficient Catalyst for the Reduction of Glutathionylated Aldehydes Derived from Lipid Peroxidation. *Free Radical Biol. Med.* **2016**, *99*, 323–332.

(39) Hauck, A. K.; Bernlohr, D. A. Oxidative Stress and Lipotoxicity. *J. Lipid Res.* **2016**, *57*, 1976–1986.

(40) Hatahet, F.; Ruddock, L. W. Substrate Recognition by the Protein Disulfide Isomerases. *FEBS J.* **2007**, *274*, 5223–5234.

(41) Seifried, A.; Schultz, J.; Gohla, A. Human HAD Phosphatases: Structure, Mechanism, and Roles in Health and Disease. *FEBS J.* **2013**, *280*, 549–571.

(42) Guo, S.; Ran, H.; Xiao, D.; Huang, H.; Mi, L.; Wang, X.; Chen, L.; Li, D.; Zhang, S.; Han, Q.; Zhou, T.; Li, A.; Man, J. NT5DC2 Promotes Tumorigenicity of Glioma Stem-like Cells by Upregulating Fyn. *Cancer Lett.* **2019**, *454*, 98–107.

(43) Xu, S.; Butkevich, A. N.; Yamada, R.; Zhou, Y.; Debnath, B.; Duncan, R.; Zandi, E.; Petasis, N. A.; Neamati, N. Discovery of an Orally Active Small-Molecule Irreversible Inhibitor of Protein Disulfide Isomerase for Ovarian Cancer Treatment. *Proc. Natl. Acad. Sci. U. S. A.* **2012**, *109*, 16348–16353.

(44) Kyani, A.; Tamura, S.; Yang, S.; Shergalis, A.; Samanta, S.; Kuang, Y.; Ljungman, M.; Neamati, N. Discovery and Mechanistic Elucidation of a Class of Protein Disulfide Isomerase Inhibitors for the Treatment of Glioblastoma. *ChemMedChem.* **2018**, *13*, 164–177.

(45) Kaplan, A.; Gaschler, M. M.; Dunn, D. E.; Colligan, R.; Brown, L. M.; Palmer, A. G.; Lo, D. C.; Stockwell, B. R. Small Molecule-Induced Oxidation of Protein Disulfide Isomerase Is Neuroprotective. *Proc. Natl. Acad. Sci. U. S. A.* **2015**, *112*, E2245–52.

(46) Rana, P.; Naven, R.; Narayanan, A.; Will, Y.; Jones, L. H. Chemical Motifs That Redox Cycle and Their Associated Toxicity. *MedChemComm* **2013**, *4*, 1175.

(47) Bekendam, R. H.; Bendapudi, P. K.; Lin, L.; Nag, P. P.; Pu, J.; Kennedy, D. R.; Feldenzer, A.; Chiu, J.; Cook, K. M.; Furie, B.; Huang, M.; Hogg, P. J.; Flaumenhaft, R. A Substrate-Driven Allosteric Switch That Enhances PDI Catalytic Activity. *Nat. Commun.* **2016**, *7*, 12579.

(48) Chakravarthi, S.; Jessop, C. E.; Bulleid, N. J. The Role of Glutathione in Disulphide Bond Formation and Endoplasmic-Reticulum-Generated Oxidative Stress. *EMBO Rep.* **2006**, *7*, 271–275.